

Glancing incidence x-ray fluorescence spectrometry based on a single-bounce parabolic capillary

Shangkun Shao(邵尚坤), Huiquan Li(李惠泉), Tianyu Yuan(袁天语), Xuepeng Sun(孙学鹏), Lu Hua(华路), Zhiguo Liu(刘志国), and Tianxi Sun(孙天希)

Citation: Chin. Phys. B, 2023, 32 (**8**): 080702. DOI: 10.1088/1674-1056/ac9b38
Journal homepage: http://cpb.iphy.ac.cn; http://iopscience.iop.org/cpb

What follows is a list of articles you may be interested in

A method for calibrating the confocal volume of a confocal three-dimensional micro-x-ray fluorescence setup

Peng Zhou(周鹏), Xin-Ran Ma(马欣然), Shuang Zhang(张爽), Tian-Xi Sun(孙天希), Zhi-Guo Liu(刘志国)
Chin. Phys. B, 2020, 29 (**2**): 020702. DOI: 10.1088/1674-1056/ab671c

Anisotropic total variation minimization approach in in-line phase-contrast tomography and its application to correction of ring artifacts

Dong-Jiang Ji(冀东江), Gang-Rong Qu(渠刚荣), Chun-Hong Hu(胡春红), Bao-Dong Liu(刘宝东), Jian-Bo Jian(简建波), Xiao-Kun Guo(郭晓坤)
Chin. Phys. B, 2017, 26 (**6**): 060701. DOI: 10.1088/1674-1056/26/6/060701

An *in situ* high-pressure X-ray diffraction experiment of hydroxyapophyllite

Fan Da-Wei (范大伟), Wei Shu-Yi (魏舒怡), Xie Hong-Sen (谢鸿森)
Chin. Phys. B, 2013, 22 (**1**): 010702. DOI: 10.1088/1674-1056/22/1/010702

Glancing incidence x-ray fluorescence spectrometry based on a single-bounce parabolic capillary

Shangkun Shao(邵尚坤)[1,2], Huiquan Li(李惠泉)[1,2], Tianyu Yuan(袁天语)[1,2], Xuepeng Sun(孙学鹏)[1,2], Lu Hua(华路)[1,2], Zhiguo Liu(刘志国)[1,2], and Tianxi Sun(孙天希)[1,2,†]

[1] *Key Laboratory of Beam Technology of the Ministry of Education, College of Nuclear Science and Technology, Beijing Normal University, Beijing* 100875, *China*

[2] *Institute of Radiation Technology, Beijing Academy of Science and Technology, Beijing* 100875, *China*

(Received 27 August 2022; revised manuscript received 10 October 2022; accepted manuscript online 19 October 2022)

Glancing incidence x-ray fluorescence spectrometry using a single-bounce parabolic capillary is proposed for the analysis of layered samples. The divergence of the x-ray beam was 0.33 mrad. In this paper, we used this instrumental setup to analyze a Si single crystal and a 50 nm HfO_2 single-layer film deposited on a Si substrate.

Keywords: single-bounce parabolic capillary, glancing incident x-ray fluorescence (GIXRF), atomic layer deposition, film analysis

PACS: 07.85.Tt, 07.85.Qe **DOI:** 10.1088/1674-1056/ac9b38

1. Introduction

X-ray fluorescence (XRF) spectrometry is an established analytical tool for detecting trace amounts of material on a micrometer depth scale.[1,2] It has been applied in several research fields, such as chemical analysis,[3] mineral analysis,[4] archaeometry,[5] medicine,[6] jewelry identification[7] and environmental sciences.[8,9] In conventional XRF spectrometry, the angle of incidence of the primary x-ray beam is usually set to around 45° to study the properties of relatively deep regions of the sample. However, the nanoscale depth properties of samples cannot be obtained using conventional XRF spectrometry.

Grazing incidence x-ray fluorescence (GIXRF) analysis is a nondestructive technique on a nanometer depth scale that can measure nanoscale depth properties of samples, such as elemental composition, concentration profile and the thickness and density of surface layers. In GIXRF spectrometry, the grazing incidence x-ray beam interferes with the x-ray beam reflected by the smooth sample, and an x-ray standing wave (XSW) field is formed above the reflective surface, which modifies the XRF excitation intensity.[10] The fluorescence yield is associated with the XSW field. In order to benefit from the enhancement of the interference effect resulting from the formation of an XSW, the grazing incidence x-ray beam on the sample usually has low divergence and is monochromatic.[11] The range of grazing incidence angle varies depending on the energy of the x-rays and the test sample, and is usually from 0° up to three or four times the total reflection critical angle.

A conventional GIXRF spectrometer has two types of x-ray optics systems to acquire a suitable low-divergence monochromatic grazing incidence x-ray beam. One is the combination of a filter and double-slit system and the other is a monochromator (crystal) and single-slit system. However, these two x-ray optical systems for GIXRF spectrometers may result in a loss of x-ray intensity, which increases the experimental time. In order to reduce the loss of x-ray intensity, Yang *et al.*[12] proposed an x-ray optics system for GIXRF technology, which consists of a parallel polycapillary x-ray lens (PPXRL) and a filter. In this experimental setup, a 0.02 mm×0.05 mm microbeam was obtained using two slits. Although a GIXRF spectrometer based on PPXRL can effectively reduce the loss of x-ray intensity it has a relatively large divergence of 0.6 mrad, which is related to the multiple total reflections of x-rays in PPXRL. The output divergence β from a capillary of a PPXRL is approximately given by the total reflection critical angle at the inner wall of the capillary, and therefore depends on the x-ray energy,[13] as show in Fig. 1.

A single-bounce parabolic capillary (SBPC) is an important single total reflection type x-ray optical device that can reflect the divergent x-ray beam into a quasi-parallel x-ray beam, and there is no output divergence β caused by multiple total reflections (Fig. 1). Therefore, it can obtain a higher-quality parallel x-ray beam than a PPXRL for GIXRF analysis. In addition, its transmission efficiency is higher than that of a PPXRL, at about six times that of a PPXRL. A SBPC also eliminates the low-energy background and high-energy component of the primary x-ray spectrum.[12]

In this paper, we propose the use of a SBPC to perform GIXRF analysis of a layered sample. The performance of this GIXRF spectrometer is presented, and application of this GIXRF technology in analysis of a 50 nm HfO_2 single layer deposited on a Si substrate is studied.

†Corresponding author. E-mail: stx@bnu.edu.cn

© 2023 Chinese Physical Society and IOP Publishing Ltd

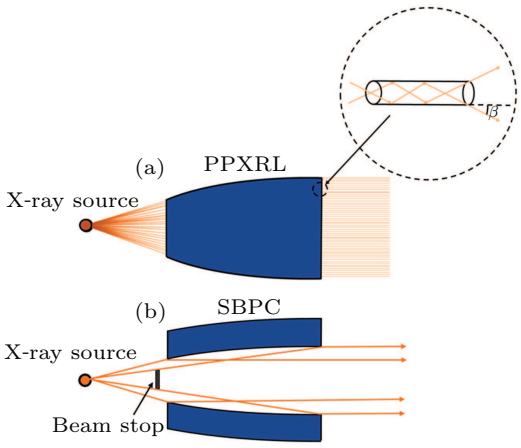


Fig. 1. Sketches of x-ray reflections from (a) a PPXRL and (b) a SBPC.

2. Experiment

Figure 2 shows a schematic diagram of the GIXRF spectrometer with a SBPC. The x-ray source is a Mo rotating-anode x-ray generator with a spot size of 300 μm×300 μm. In the experiment the operating voltage and current were 35 kV and 50 mA, respectively. A Nb filter placed between the source and the SBPC was used to obtain monochromatic incident x-rays (Mo $K\alpha$). A beam stop in front of the SBPC was used to block the incident x-rays that were not reflected by the SBPC, and a pinhole of 0.02 mm×0.6 mm consisting of two slits was placed in front of the sample to narrow the x-ray beam emerging from the SBPC. The sample was adjusted by a motorized X–Y–Z–R stage. A silicon drift detector (SDD) with a sensitive area of 80 mm^2 was used to detect x-ray fluorescence (its energy resolution was less than 139 eV at 5.9 keV). The input focal length L_1 is the distance from the x-ray source to the entrance of the SBPC. The transmission efficiency of x-rays through the SBPC, η, can be expressed as

$$\eta = \frac{I_{\text{out}}}{I_{\text{in}}}, \tag{1}$$

where I_{in} is the x-ray intensity entering the SBPC with a beam stop and I_{out} is the x-ray intensity emitted from the exit of the SBPC.

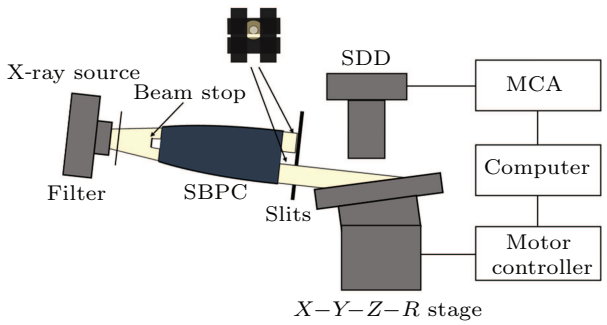


Fig. 2. Schematic diagram of the GIXRF setup with a SBPC.

3. Results and discussion

3.1. SBPC

The parameters of the SBPC are presented in Table 1. The length of the SBPC is 100.0 mm. Figure 3 shows microscopic cross-sectional images of the entrance and exit of the SBPC. The surface error of the SBPC is mainly diameter error and centerline error. In order to evaluate the quality of a SBPC, a constant ratio method of inner and outer diameters based on a digital micrometer was used to obtain the diameter error

Table 1. Parameters of SBPC.

Parameters	SBPC
Input focal length L_1 (mm)	200.0
Length L (mm)	100.0
Input diameter d_1 (mm)	1.20
Output diameter d_2 (mm)	1.47
Surface slope error (μrad root mean square)	17.96
Transmission efficiency η (%)	87.80

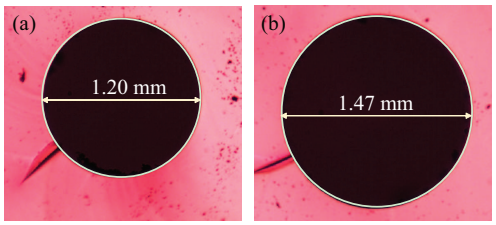


Fig. 3. (a) Input diameter d_1 of the SBPC. (b) Output diameter d_2 of the SBPC.

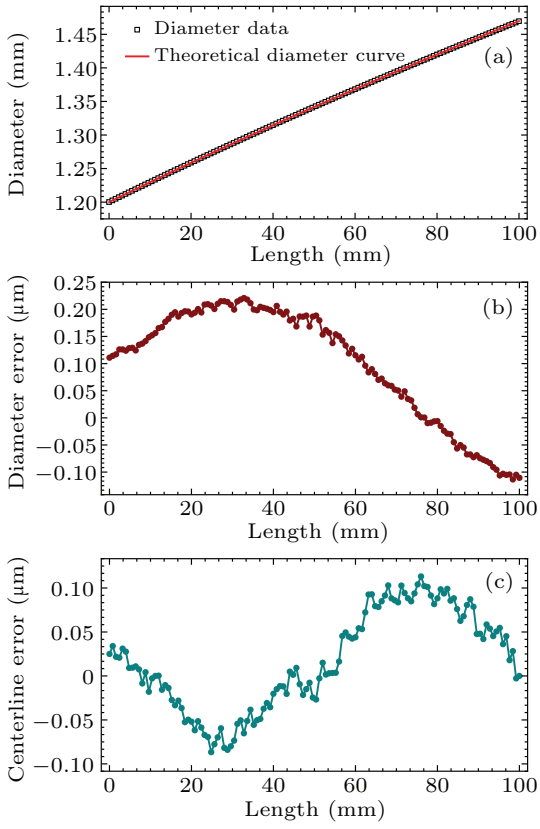


Fig. 4. (a) Comparison of the theoretical diameter of the SBPC with measured data. (b) Diameter error of the SBPC. (c) Centerline error of the SBPC.

and centerline error. A detailed introduction to this method is given by Sun *et al.*[14] Figure 4(a) compares the theoretical diameter of the SBPC with the measured data. The red curve is the ideal diameter curve for the SBPC and the black squares are the measured data obtained by the digital micrometer. Figures 4(b) and 4(c) show the diameter error and centerline error curves of the SBPC, respectively. The total surface slope error can be obtained from the diameter error and centerline error, and its root mean square is 17.96 μrad.

3.2. Beam divergence of the SBPC

In order to evaluate the divergence of a beam incident on the sample, a knife edge scan method was used to measure the width of the x-ray beam at different positions along the direction of the incident x-rays. A detailed introduction to this method is given by Yang *et al.*[12]

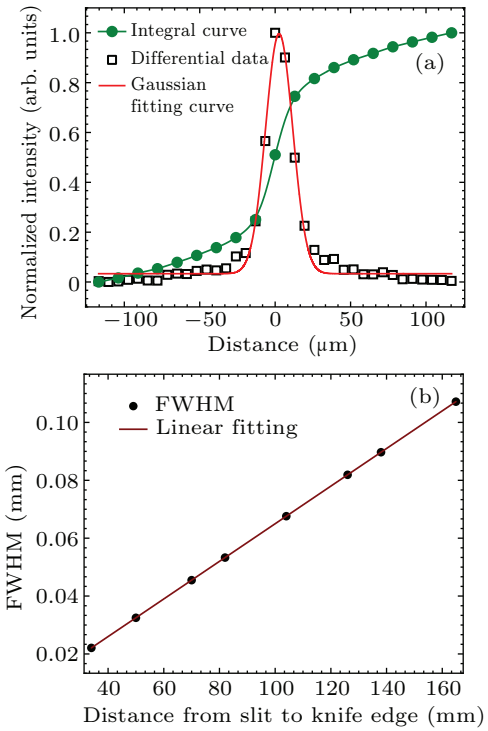


Fig. 5. (a) The vertical intensity distribution curve of the x-ray beam obtained by the knife edge scanning method. (b) Relationships between the x-ray beam width and the position of the knife edge.

Figure 5(a) shows the result of the knife edge scan obtained at a distance of 34 mm between the slit and the knife edge. The green curve is the normalized integral intensity curve obtained by the knife edge scan method. The black circles are the differential data corresponding to the green curve, and the red curve is the Gaussian fitting curve of the differential data with a full width at half maximum (FHWM) of 21.28 μm. The vertical normalized intensity distribution of the x-ray beam emerging from the slits is approximately a Gaussian distribution. The x-ray beam width is the FHWM of the Gaussian fitting function. X-ray beam widths were obtained at eight different locations, as shown in Fig. 5. The divergence of the x-ray beam incident on the sample was calculated as 0.33 mrad by linearly fitting the x-ray beam widths at different positions; this was smaller than the divergence of the GIXRF setup with a PPXRL. There are two main reasons for the divergence of x-rays emitted from a SBPC: one is the focal spot size of the x-ray source and the other is the surface slope error of the SBPC.

3.3. Evaluation of the stability of the GIXRF setup with a SBPC

In order to obtain better counting statistics and a shorter experimental time, the scan step size used was 0.0125° and the detection time of each scan step was 30 s. A Si single crystal was used to optimize the sample position and grazing incidence angle for the GIXRF spectrometer, and the optimized XRF-normalized intensity spectrum of the Si single crystal is shown in Fig. 6. The Si $K\alpha$ fluorescence intensity changes drastically around the angle $\theta_{c,Si} = 1.74$ mrad, which is related to the energy of the incident x-rays. In order to evaluate the stability of this GIXRF setup with a SBPC, we repeated the detection of the Si single crystal ten times, and the standard deviation of the angle $\theta_{c,Si}$ was 0.02 mrad. Therefore, this GIXRF setup with a SBPC had good testing repeatability.

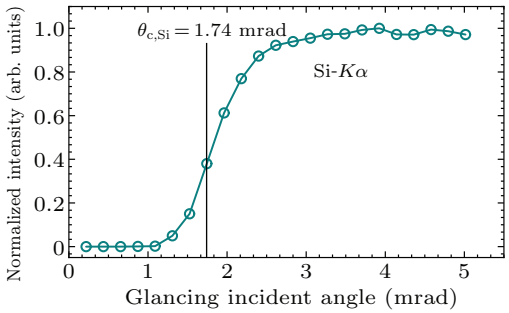


Fig. 6. Glancing angle dependence of normalized intensity for a Si single crystal.

3.4. Application of a SBPC in GIXRF analysis of a HfO_2 single-layer film

The scanning electron microscopy image of the cross section of a HfO_2 single-layer film is shown in Fig. 7. The HfO_2 single layer was deposited on a Si substrate by atomic layer deposition and its thickness was about 50 nm. The glancing angle dependence of normalized intensity for a HfO_2 single-layer film is shown in Fig. 8. The Hf $L\alpha$ fluorescence intensity increased dramatically around the angle $\theta_{c,Hf} = 3.27$ mrad. The density of the HfO_2 single layer can be given by

$$\rho = \frac{\pi \sum_i w_i A_i}{r_e N_A \sum_i w_i f_{1,i}} \cdot \theta_c^2 \cdot E^2 \approx 9.63 \text{ g/cm}^3, \quad (2)$$

where E is the energy of incident x-rays (17.4 keV), N_A is the Avogadro constant, w_i is the proportion of HfO_2 atoms i, A_i is the atomic weight of HfO_2 atoms i, r_e is the classical electron radius and $f_{1,i}$ is the real part of the anomalous atomic form

factor f, which can be obtained from the NIST website.[15] As shown in Fig. 8, the ripples in the GIXRF spectra are caused by interference of the grazing incidence x-ray beam and the reflected beam, and these ripples are one of the main features of GIXRF spectra. According to GIXRF theory, the intensity of x-ray fluorescence is related to the thickness of the layered sample. Therefore, GIXRF technology is an effective analytical method for the density and thickness of layered samples.

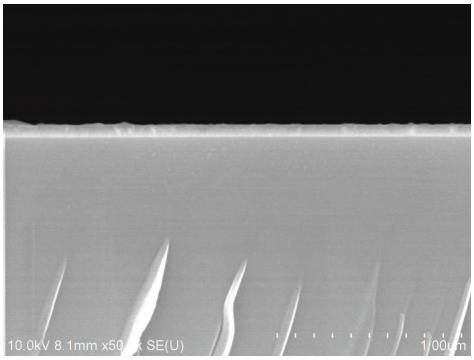


Fig. 7. Scanning electron microscope image of the cross-section of a HfO_2 single-layer film deposited on a Si substrate.

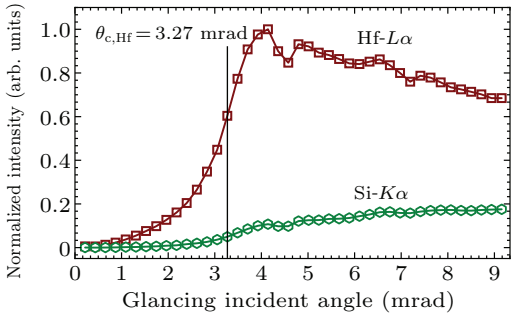


Fig. 8. Glancing angle dependence of normalized intensity for a HfO_2 single layer deposited on a Si substrate.

4. Conclusion and perspectives

In this research, a newly developed GIXRF spectrometer using a SBPC was applied for the analysis of layered samples. The evaluated divergence of the x-ray beam was 0.33 mrad. The SBPC can eliminate low-energy background and the high-energy component of the primary x-ray spectrum. Divergence of the SBPC increases with the spot size of the x-ray source, so in order to achieve the low divergence required for GIXRF analysis, the SBPC was designed with a large input focal length L_1, which increased the loss of the x-ray beam. Two approaches have been proposed to solve this problem: one is to use a SBPC coated with a high-density material to increase the x-ray total reflection critical angle and thus increase the receiving solid angle; the other is to use a microfocus x-ray source, which allows a SBPC to be designed with a small input focal length L_1. Both these approaches can increase the intensity of x-rays incident on the sample, and also ensure that the x-ray beam has a low divergence.

Acknowledgements

Thanks to Yanli Li (Institute of Electrical Engineering, Chinese Academy of Sciences) for the providing the HfO_2 single-layer film.

Project supported by the National Key Research and Development Program of China (Grant No. 2021YFF0701202), and the National Natural Science Foundation of China (Grant No. 11875087).

References

[1] Lin X Y, Wang Z H, Chu X L, Sun T X and Ding X L 2007 *Chin. Phys Lett.* **24** 3368
[2] Li Y L, Wang Y B, Lu W E, Kong X D, Han L and Zhao H B 2021 *Chin. Phys. B* **30** 050703
[3] Peng S, Liu Z, Sun T, Wang G, Ma Y and Ding X 2014 *Appl. Radiat. Isot.* **90** 84
[4] D'Angelo J, Perino E, Marchevsky E and Riveros J A 2002 *X-ray Spectrom.* **31** 419
[5] Wolff T, Rabin I, Mantouvalou I, Kanngiesser B, Malzer W, Kindzorra E and Hahn O 2012 *Anal. Bioanal. Chem.* **402** 1493
[6] Nyga A, Cheema U and Loizidou M 2011 *J. Cell Commun. Signal* **5** 239
[7] Karydas A, Kotzamani D, Bernard R, Barrandon J N and Zarkadas C 2004 *Nuclear Instruments and Methods in Physics Research B* **226** 15
[8] Vincze L, Somogyi A, Osan J, Vekemans B, Torok S, Janssens K and Adams F 2002 *Anal. Chem.* **74** 1128
[9] Zimmermann F, Ebert M, Worringen A, Schutz L and Weinbruch S 2007 *Atmos. Environ.* **41** 8219
[10] Hönicke P, Beckhoff B, Kolbe M, Giubertoni D, van den Berg J and Pepponi G 2010 *J. Analytical Bioanalytical Chemistry* **396** 2825
[11] Szwedowski-Rammert V, Baumann J, Schlesiger C, Waldschlager U, Gross A, Kanngiesser B and Mantouvalou I 2019 *J. Anal. At. Spectrom.* **34** 922
[12] Yang J, Zhao D, Xu Q and Ding X 2009 *Appl. Surf. Sci.* **255** 6439
[13] MacDonald C A 2010 *X-ray Optics and Instrumentation* **2010** 17
[14] Sun X, Zhang X, Wang Y, Shao S, Li Y, Peng S, Liu Z and Sun T 2020 *Spectrochimica Acta Part B: Atomic Spectroscopy* **165** 105770
[15] See for the "Basic Information" (last accessed May 15, 2022)